Applied Physics Letters ARTICLE scitation.org/journal/apl

Enhancement of light-induced resistance effect in the nanostructure of Ag/graphene based on the n-type silicon

Cite as: Appl. Phys. Lett. **119**, 061104 (2021); doi: 10.1063/5.0062661
Submitted: 7 July 2021 · Accepted: 5 August 2021 ·
Published Online: 12 August 2021

Shuai Liu,[1,a)] Xinyuan Dong,[2] Yiru Niu,[2] Diyuan Zheng,[2] Zhikai Gan,[3] and Hui Wang[2,a)]

AFFILIATIONS

[1]School of Science, North University of China, No. 3, Xueyuan Road, Taiyuan, Shanxi 030051, China
[2]State Key Laboratory of Advanced Optical Communication Systems and Networks, School of Physics and Astronomy, and Key Laboratory for Thin Film and Microfabrication Technology of the Ministry of Education, Research Institute of Micro/Nano Science and Technology, Shanghai Jiao Tong University, 800 Dongchuan Rd., Shanghai 200240, China
[3]Key Laboratory of Infrared Imaging Materials and Detectors, Shanghai Institute of Technical Physics, Chinese Academy of Sciences, 500 Yutian Road, Shanghai 200083, China

[a)]**Authors to whom correspondence should be addressed:** billliu198826@hotmail.com and huiwang@sjtu.edu.cn

ABSTRACT

The direct coupling of material properties across a nanoscale interface is a promising route to achieve the functionality unavailable in bulk materials. Graphene is a kind of sp2 hybridized carbon monolayer and has been investigated in many applications due to its high charge-carrier mobility. In this paper, a type of enhanced light-induced resistance effect (LRE) is observed in the structure of Ag/graphene/n-type Si. This effect features a remarkable linear resistance change with a sensitivity of 4.39 kΩ/mm when a laser moves along the surface of the structure. With the optimal thickness of the Ag film, the resistance change ratio of LRE can reach 472%, which is significantly higher than the Ag/Si control sample (6.4%), showing an obvious graphene-induced enhancement. Photocarriers' diffusion and recombination at the heterojunction interface are crucial for the enhancement. These findings offer an effective way to study the carrier dynamics at the heterojunction interface and will be useful in the development of graphene-based optoelectronic devices, such as laser-controlled variable resistors, laser-induced diodes, and storage devices.

Effective manipulation of the resistance is an old and fascinating topic that has attracted tremendous interest owing to its huge potential for various applications. Although extensive investigations have been reported on resistance effects, such as superconductivity effect,[1–6] magneto-resistance effect,[7–12] and electric-pulse-induced resistance switching effect,[13–18] attempts to control the resistance have led to an up surge of interest in developing versatile nanoscale materials in many disciplines. Graphene is an sp2 hybridized carbon monolayer[19] and has been proven to be a charming platform suitable for a broad range of nanoelectronics applications due to its extraordinary electronic properties, such as high charge-carrier mobility.[20–25] For many applications, it is desirable to obtain a linear change in resistance in the graphene-based structure.

In our previous reports,[26–31] we developed a laser-based method to control the resistance in a given metal/oxide/semiconductor (MOS) structure. In this Letter, a type of graphene interface induced enhancement of the light-induced resistance effect (LRE) is observed in the nanofilm of Ag/graphene/n-type Si. The resistance can linearly change with the laser spot position. Two most significant features of this LRE are an excellent spatial sensitivity and a large resistance change ratio as a laser moves along the surface of the structure. With the optimal thickness of an Ag film, the change ratio of resistance can reach 472%, which is much higher than the Ag/Si control sample (6.4%). Graphene is crucial for the enhancement. It not only hinders the recombination between photoholes and photoelectrons but also modulates the resistance of structure for a suitable lateral diffusion of photoelectrons. These results show that the combination of LRE with graphene is useful for applications and may add the functionality to the graphene based optoelectronic devices, such as laser-controlled variable resistors, laser-induced diodes, and storage devices.

In our experiment, substrates used in experiments are s-type monocrystalline Si (111). The thickness of the Si is around 0.3 mm,

and the resistivity is within the range of 50–80 Ω cm at room temperature. The native surface oxide layer of the Si was removed by a dip in dilute HF (1%). Then, Si substrates were cut into rectangles ($10 \times 10\,mm^2$). The graphene was fabricated on copper substrates by chemical vapor deposition[32] and was transferred onto the Si substrate by a polymer assisted transfer method.[33] Then, Ag nanofilms were manufactured by DC magnetron sputtering Ag (99.99%) on top of the pretreated graphene/Si substrate. During the deposition, the base pressure of the vacuum system was 1.7×10^{-4} Pa and the pressure of argon gas was 0.75 Pa. The DC power was fixed at 15 W and deposition rate of Ag was about 1.0 Å/s, which was measured by the stylus profile meter on thick calibration samples prepared under the same sputtering condition. The nominal thicknesses of fabricated films were controlled by adjusting the sputtering time. Due to the commonly existed island-growth of sputtering, nominal thickness is utilized to describe the discrete nanoclusters for a very thin Ag layer. All the contacts (less than 1 mm in diameter) to the film were formed by alloying indium with copper wires. Experimental details on fabrication are similar with our published papers.[34–39]

First, we measured the current–voltage characteristics of different structures of Ag/graphene/Si under the dark condition with Keithley 4200 by sweeping the voltage. The measurement diagram is shown in Fig. 1(a). Contacts A and B were on the metal film, and AB distance (L) was fixed at 2 mm. In Fig. 1(b), it can be easily found that inserting the graphene layer into the structure of Ag/Si can decrease the resistance. As the thickness of Ag film gets larger, the resistance becomes lower. The inset shows photography of sample and scanning electron microscopy images (top view) of the Ag unfully covered nanofilm with a nominal thickness of 1 nm.

Then, we investigated the LRE of Ag(1 nm)/graphene/Si under a 30 W, 635 nm laser illumination focused on a roughly 50 μm diameter spot at the metal surface. The local temperature of the spot is around room temperature. Cares were taken to avoid any spurious illumination (e.g., background light) reaching the sample. Figure 2(a) shows the diagram of energy bands of Ag/graphene/Si, where $\chi_{n\text{-}Si}$ is the electron affinity (4.05 eV), Eg is the energy gap of Si (1.1 eV), Φ_G is the work function of graphene (4.7 eV), and Φ_{Ag} is the work function of silver (4.26 eV). When the laser impinges at the surface of materials, the electron–hole pairs are generated inside the silicon, and soon, these excited electrons will be tunneled through the graphene into the metallic film of Ag. The LRE measurement diagram is shown in Figs. 2(b) and 2(c). R_P represents the resistance with a positive bias (A−, B+), and R_N represents the resistance with a negative bias (A+, B−).

As shown in Fig. 2(d), when L is fixed at 2 mm, R_P linearly increases with laser position and R_N linearly decreases with laser position, as we move the laser from contact A to contact B. For dark condition, resistance remains unchanged (7.3 kΩ). When laser position is at the midpoint of AB, R_P is same as R_N with a resistance of 6.6 kΩ. Considering the metallic nature of the film, the resistance is quite high. It may originate from the Ag unfully covered nanofilm [as shown in Fig. 1(b)] and defects near the interface of Ag/graphene. The Ag unfully covered nanofilm cannot provide a whole channel for electron transport. During the lateral transport, electrons always need to transit through Ag nanoparticles to graphene. It enhances the scattering probability between defects and electrons, increasing the resistance.

Due to the linear change in resistance with laser position, sensitivity of LRE is defined as the variation of resistance when the laser moves a unit distance (always 1 mm).[26,28] Sensitivity of R_P and R_N both is about 4.39KΩ/mm. In addition, we also investigated LRE sensitivity dependence on the AB distance (L) and laser power (P), as shown in Fig. 2(e). With a fixed L of 2 mm, the sensitivity is proportional to the laser power and increases to 4.39 kΩ/mm as P reaches a maximum of 30mW. With a fixed P of 30 mW, a larger L leads to a smaller sensitivity that exponentially decays with L. Furthermore, by varying the thickness of the Ag film (d_{Ag}), we find that the sensitivity has a great bearing on the thickness. As d_{Ag} gets away from 1 nm, the sensitivity dramatically decreases as shown in Fig. 2(f).

In addition, we measure the current–voltage characteristics for different laser positions in Fig. 3(a). I–V curve in the negative bias region (R_N measurement) corresponds to a high resistance with illumination on A (a low resistance with illumination on B), and I–V curve in the positive bias region (R_P measurement) corresponds to a low resistance with illumination on A (a high resistance with illumination on B). For the illumination on midpoint, the slope of I–V curve in the negative bias region is similar to that in the positive bias region.

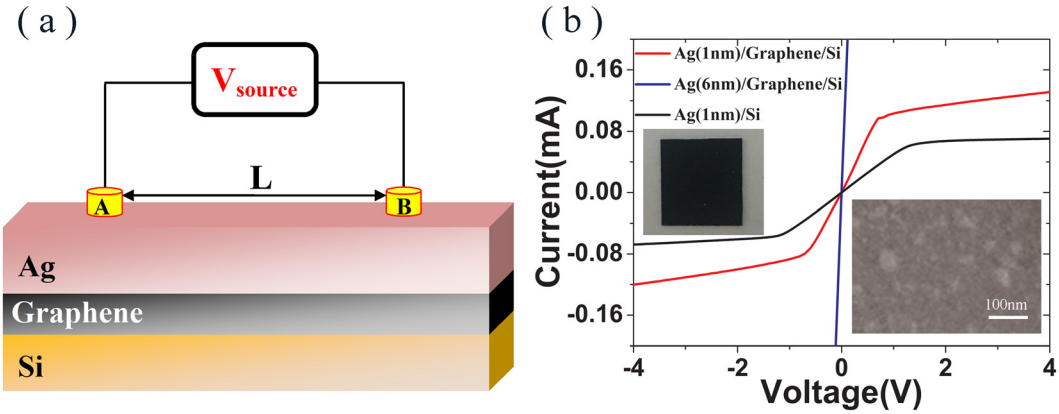

FIG. 1. (a) Current–voltage characteristics measurement diagram with Keithley 4200. A and B are two Ohmic contacts. (b) Current–voltage characteristics of different structures for a fixed AB distance of 2 mm with the dark condition. Inset: photography of the sample and scanning electron microscopy images (top view) of the Ag unfully covered nanofilm.

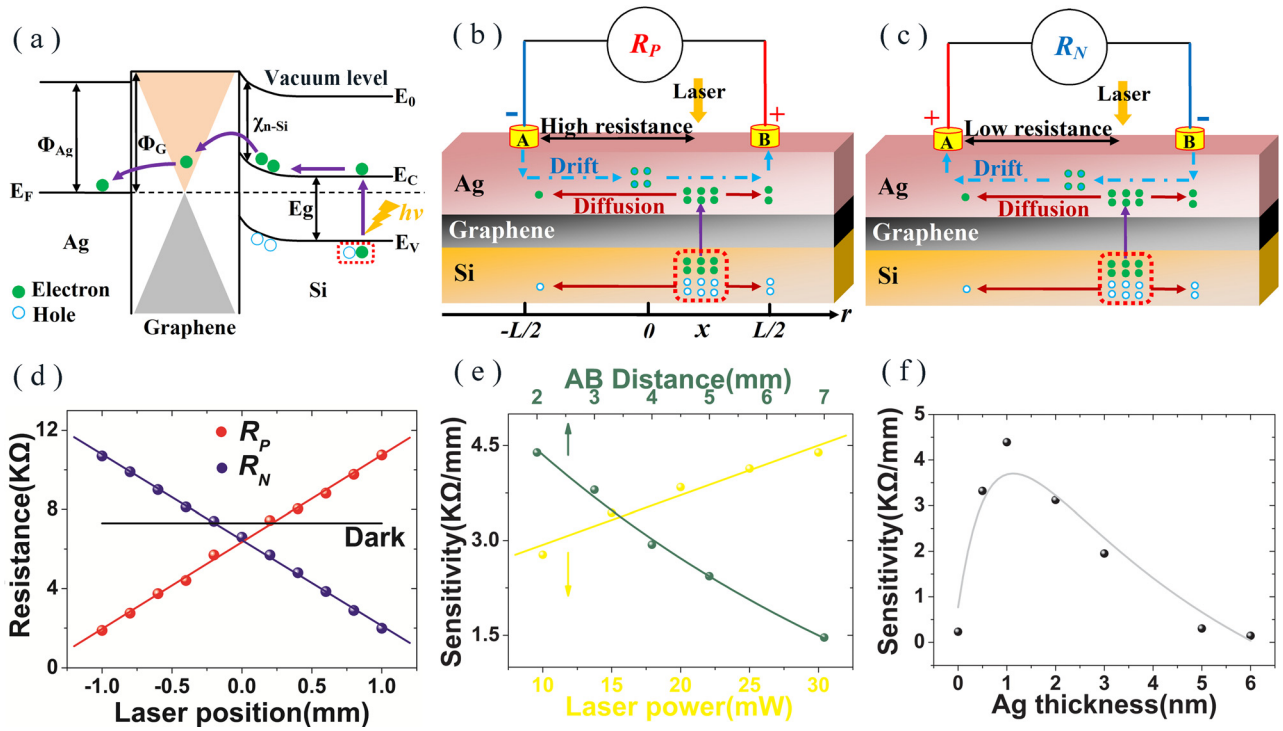

FIG. 2. (a) Diagram of energy bands of Ag/graphene/Si. (b) R_P measurement diagram with a positive bias (A-, B+). Laser keeps moving between two contacts. (c) R_N measurement diagram with a negative bias (A+, B−). (d) LRE in the structure of Ag(1 nm)/graphene/Si with a fixed AB distance(L) of 2 mm and laser power (P) of 30 W. Black line represents for the dark condition. (e) The sensitivity as a function of laser power and AB distance in the structure of Ag(1 nm)/graphene/Si. The olive line is exponential decay fit, and the yellow line is the linear fit. (f) The sensitivity as a function of Ag nominal thickness in the Ag/graphene/Si structure. The gray line is the theoretical fit line.

Moreover, we measure the resistivity of AB with a four-electrode system, as shown in Fig. 3(b). Inset shows the four-electrode measurement diagram. Steady current source is applied between contacts C and D. The steady current is kept as 0.1 mA for illumination condition and is kept as 0.01 mA for the dark condition due to the voltage high limit. Voltmeter is applied between contacts A and B. CA = AB = BD = L. As for linear four electrodes, resistivity (ρ) can be described as Eq. (1), where V_{AB} is the voltage between A and B, I is the steady current, and r_{ij} (i,j = A–D) is the distance between two electrodes,

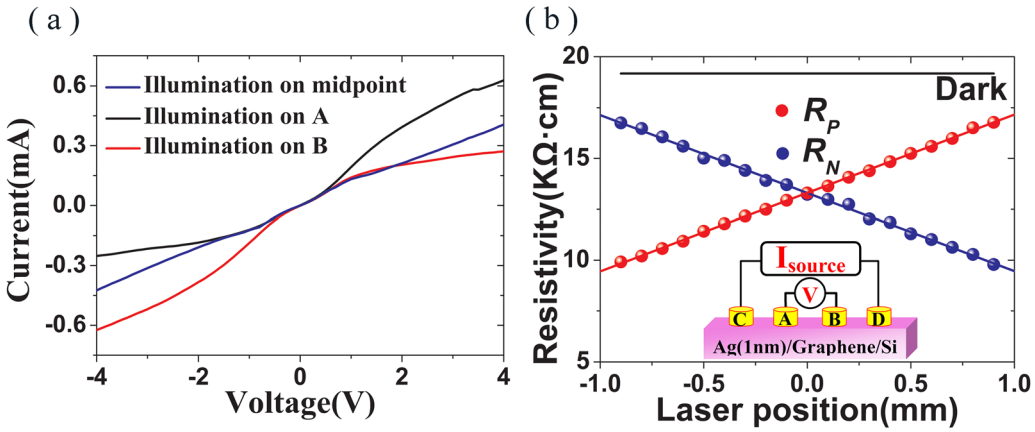

FIG. 3. (a) Current–voltage characteristics of different laser positions in the structure of Ag(1 nm)/graphene/Si with a fixed AB distance (L) of 2 mm and laser power (P) of 30 W. (b) Resistivity (ρ) of the four-electrode system in the structure of Ag(1 nm)/graphene/Si with a fixed AB distance (L) of 2 mm and laser power (P) of 30 W. R_P represents for a positive current flow (D → C), and R_N represents for a negative current flow (C → D). Black line represents for the dark condition. Inset: Four-electrode measurement diagram. Laser keeps moving between two contacts A and B.

$$\rho = \frac{2\pi V_{AB}}{I}\left(\frac{1}{r_{CA}} - \frac{1}{r_{AD}} - \frac{1}{r_{CB}} + \frac{1}{r_{BD}}\right)^{-1} = \frac{2\pi L V_{AB}}{I}. \quad (1)$$

Resistivity linearly changes with the laser position, which is similar to the two electrode system's results. In the R_P measurement condition, current flows from D to C (drift electrons flow from C to D). When laser illuminates on contact A, resistivity is lowest (9.8 kΩ cm). When laser illuminates on contact B, resistivity is highest (16.7 kΩ cm). As for the R_N measurement condition, resistivity linearly decreases, which is opposite to the R_P measurement condition. R_P is same to R_N with illumination on the midpoint (13.3 kΩ cm). The resistivity of the dark condition remains unchanged (19.2 kΩ cm).

The LRE mechanism can be described as the extra scattering between photoelectrons and drift electrons, as shown in Figs. 2(b) and 2(c). The density of photoelectrons at the illuminated laser spot is the highest and can create a gradient laterally between the illuminated and the non-illuminated zones, resulting in the photoelectrons diffusion. The region of high resistance is the area where the direction of photoelectrons diffusion is opposite to the direction of drift electrons and the region of low resistance is the area where the direction of photoelectrons diffusion is same as the direction of drift electrons. As we move the laser, the size of high resistance region and low resistance region can be controlled by the laser position. Thus, we can modulate (increase or decrease) the resistance by the laser. What is more, if laser spot gets larger, initial density of photoelectrons will become smaller, weakening the lateral diffusion and LRE.

According to our previous work,[26] the density of diffusion electrons $n(r)$ can be written as

$$n(r) = n_0 \exp\left(-\frac{|r-x|}{\lambda}\right). \quad (2)$$

Here, n_0 is the initial density of photoelectrons, x is the laser position, and λ is the diffusion length. Taking R_P for example, the resistance $\rho(r)$ can be written as

$$\rho(r) = \begin{cases} \rho_0\left[1 - \frac{n_0}{N_0}\exp\left(-\frac{r-x}{\lambda}\right)\right] & \left(x < r < \frac{L}{2}\right) \\ \rho_0\left[1 + \frac{n_0}{N_0}\exp\left(-\frac{x-r}{\lambda}\right)\right] & \left(-\frac{L}{2} < r < x\right). \end{cases} \quad (3)$$

Here, ρ_0 is the original resistivity of the material and N_0 is the density of drift electrons. Thus, the resistance of AB can be calculated by

$$R(x) = \int_{-\frac{L}{2}}^{\frac{L}{2}} \rho(r)dr \approx \rho_0(L + Kx). \quad (4)$$

When x satisfies $|x| \ll \lambda$, resistance can be idealized as linear change with x. Here, $\rho_0 L$ should be the original resistance of the dark condition. It can be found that resistance of the dark condition is higher than the resistance of illumination on midpoint ($x = 0$) as shown in Figs. 2(d) and 3(b). This phenomenon indicates that a part of photoelectrons still remain and contribute to the current, like a common photoresistor that resistance decreases under illumination. Hot carriers trigger by Ag-nanoparticles-induced localized surface plasmons may be another possible contributor to the photocurrent for decreasing the resistance. $\rho_0 K$ is the sensitivity that can be written as

$$Sensitivity = \rho_0 K = \frac{2\rho_0 n_0 \exp\left(-\frac{L}{2\lambda}\right)}{N_0}. \quad (5)$$

n_0 comes from total laser-generated photons and can be described as $CP/(h\nu)$, where C is a proportional coefficient, P is laser power, h is Planck constant, and ν is photon's frequency. Thus, we can get the sensitivity as a function of P and L in the following equation:

$$Sensitivity(P, L) = \frac{2\rho_0 CP \exp\left(-\frac{L}{2\lambda}\right)}{N_0 h\upsilon}. \quad (6)$$

From Eq. (6), it can be easily found that sensitivity increases with P linearly and decays with L exponentially, which is consistent with Fig. 2(e).

The "thickness effect" in Fig. 2(f) can be understood by the variation of electron diffusion length (λ). For simplicity, here we assume that λ linearly changes with d_{Ag}. $\lambda = \alpha(d_{Ag} + d_0)$, where α is a positive proportionality coefficient, d_0 is effective thickness of the graphene/Si substrate for photoelectron transport. Furthermore, we suppose that n_0 is inversely proportional to $d_{Ag} + d_0$, which means $n_0(d_{Ag} + d_0) = C'$. Here, C' is a proportional coefficient related to the total number of photoelectrons. Thus, the sensitivity as a function of d_{Ag} can be described as shown in the following equation and we get the theoretical fit line in Fig. 2(f):

$$Sensitivity(d_{Ag}) = \frac{2\rho_0 C' \exp\left[-\frac{L}{2\alpha(d_{Ag} + d_0)}\right]}{N_0(d_{Ag} + d_0)}. \quad (7)$$

To gain additional insights into this LRE observed in the structure of Ag/graphene/Si, we calculate the change ratio of resistance (Δ) defined as Eq. (8).[26,28] Δ is the main criterion for judging the performance of LRE. Δ of Ag(1 nm)/graphene/Si can reach as high as 472%. As a contrast, Δ of Ag(1 nm)/Si and graphene/Si are only 6.4% and 7.7%, respectively. Although sensitivity ($\rho_0 K$) of Ag(1 nm)/graphene/Si is much lower than that of reported results (0.14–0.79 MΩ/mm) due to the low ρ_0 of Ag, Δ is higher than that of reported results (110%–280%).[28–30]

$$\Delta \equiv \frac{R_{max} - R_{min}}{R_{min}} \times 100\%. \quad (8)$$

With a similar phenomenon in Fig. 2(e), we can easily find that a higher P or a shorter L both can produce a larger Δ, as shown in Fig. 4(a). As P increases from 10 to 30 mW, Δ with a fixed L of 2 mm increases from 160% to 472%. As L increases from 2 to 7 mm, Δ with a fixed P of 30mW drops to 61%. What is more, we find that 1 nm is the optimal thickness of the Ag film for obtaining the largest Δ, as shown in Fig. 4(b). In the structure of Ag(1 nm)/graphene/Si, we measure Δ with different laser wavelengths (532, 635, 780, and 980 nm). It can be found that Δ of 635 nm is highest (315% for 532 nm, 472% for 635 nm, 437% for 780 nm, and 86% for 980 nm). Due to that power is fixed and made of energy of photon, the laser with longer wavelength can provide more photons. However, the coefficient of light absorption of Si decreases with wavelength up to cutoff wavelength. Thus, a suitable wavelength should not be too short or too long.

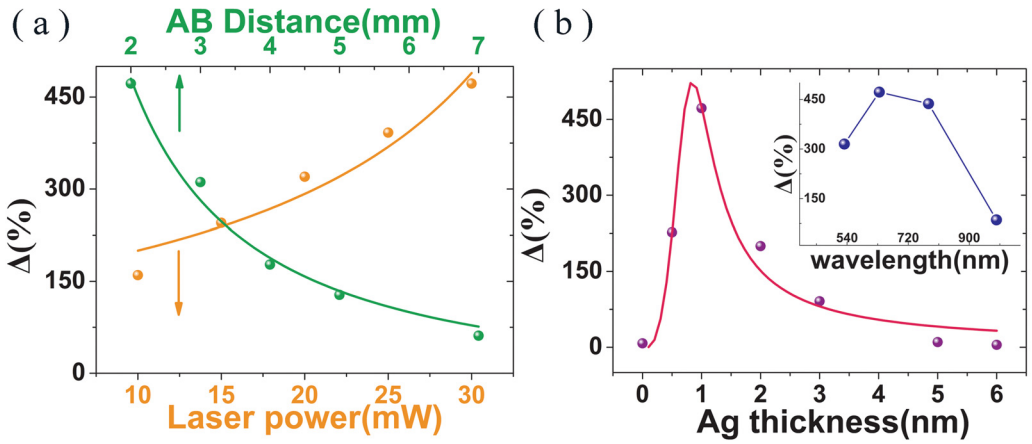

FIG. 4. (a) The change ratio of resistance as a function of laser power and AB distance in the structure of Ag(1 nm)/graphene/Si. The orange line and the green line are the theoretical fit lines. (b) The change ratio of resistance as a function of Ag nominal thickness in the Ag/graphene/Si structure. The pink line is the theoretical fit line. Inset: The change ratio of resistance for different laser wavelengths with a fixed power of 30 mW and a fixed AB distance of 2 mm in the Ag(1 nm)/graphene/Si.

According to Eqs. (4) and (6), Δ can be written as the following equation and we get the theoretical fit lines in Fig. 4(a):

$$\Delta = \frac{2K}{2-K} = \frac{2CP}{N_0 h\upsilon \exp\left(\frac{L}{2\lambda}\right) - CP}. \tag{9}$$

Meanwhile, Δ as a function of d_{Ag} can also be easily described as Eq. (10) according to Eq. (7). The theoretical fit is also consistent with the experimental results in Fig. 4(b),

$$\Delta(d_{Ag}) = \frac{2C'}{N_0(d_{Ag}+d_0)\exp\left[\frac{L}{2\alpha(d_{Ag}+d_0)}\right] - C'}. \tag{10}$$

The possible mechanism of a larger Δ in the structure of Ag/graphene/Si can be explained from two parts. First, the Ag nanofilm (1 nm) is unfully covered and photoelectron's lateral diffusion is limited in the control samples of Ag/Si. However, photoelectrons can diffuse more easily in the structure of Ag/graphene/Si due to the high charge-carrier mobility of graphene, which is consistent with the results in Fig. 1(b). Photoelectrons' scattering with drift electrons is more heavily in the structure of Ag/graphene/Si, leading to a more obvious LRE. Second, Ag nanoparticles can induce localized surface plasmons and most of the light can be trapped into plasmon excitations.[40,41] It can enhance the local electric fields and increase the absorption of light and photoelectron generation in the surrounding semiconductor, leading to a more obvious LRE. Figures 5(a) and 5(b) are simulated electric field normalized intensity results with the finite element method. As shown in Fig. 5(a), it can be easily found that local electric field around Ag nanoparticles is enhanced. Figure 5(b) shows the simulated electric field results of continuous Ag film, which cannot enhance the local electric field. Thus, Δ in the structure of Ag/graphene/Si can be much larger than that in the control samples of Ag/Si and graphene/Si.

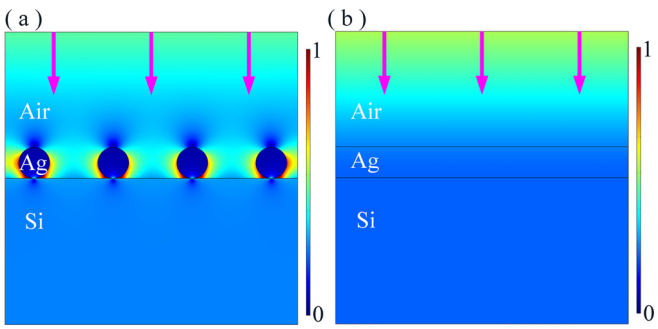

FIG. 5. (a) The simulated electric field normalized intensity results (100 × 100 nm^2) of Ag nanoparticles with the finite element method. Graphene is simulated as the surface current density at the interface between Si and Ag. Ag nanoparticles' radius is around 5.3 nm that conforms to the nominal thickness ≈ 1 nm. Magenta arrows represent the incident light of 635 nm. (b) The simulated electric field normalized intensity results of the Ag film.

In conclusion, a type of graphene interface induced enhancement of LRE is achieved in the structure of Ag/graphene/n-type Si. With the optimal thickness of the Ag film, the sensitivity can reach 4.39 KΩ/mm and the change ratio of resistance can reach 472%, much higher than the Ag/Si control sample (6.4%), showing an obvious graphene-induced enhancement. The results offer an effective way to enhance the change ratio of resistance and may stimulate both theoretical and experimental efforts in exploiting the potential applications of graphene-based memory devices.

The authors acknowledge the financial support of the National Natural Science Foundation of China (Nos. 61574090, 11874041, 11374214, 10974135, 62004203, and 61705200); the Natural Science Foundation of Shanxi Province, China (Nos. 201601D021020 and 201901D111180); Science Foundation of North University of China (No. XJJ201903); and Scientific and Technological Innovation Programs of Higher Education Institutions in Shanxi (No. 2020L0310).

DATA AVAILABILITY

The data that support the findings of this study are available from the corresponding authors upon reasonable request.

REFERENCES

[1]X. B. Lu, P. Stepanov, W. Yang, M. Xie, M. A. Aamir, I. Das, C. Urgell, K. Watanabe, T. Taniguchi, G. Y. Zhang, A. Bachtold, A. H. MacDonald, and G. K. Efetov, Nature **574**, 653 (2019).
[2]G. R. Chen, A. L. Sharpe, P. Gallagher, I. T. Rosen, E. G. Fox, L. L. Jiang, B. S. Lyu, H. Y. Li, K. Watanabe, T. Taniguchi, J. Jung, Z. W. Shi, D. Goldhaber-Gordon, Y. B. Zhang, and F. Wang, Nature **572**, 215 (2019).
[3]N. Reyren, S. Thiel, A. D. Caviglia, L. Fitting Kourkoutis, G. Hammerl, C. Richter, C. W. Schneider, T. Kopp, A. S. Rüetschi1, D. Jaccard, M. Gabay, D. A. Muller, J. M. Triscone, and J. Mannhart, Science **317**, 1196 (2007).
[4]V. V. Struzhkin, M. I. Eremets, W. Gan, H. K. Mao, and R. J. Hemley, Science **298**, 1213 (2002).
[5]Y. Y. Pai, H. Lee, J. W. Lee, A. Annadi, G. Cheng, S. Lu, M. Tomczyk, M. Huang, C. B. Eom, P. Irvin, and J. Levy, Phys. Rev. Lett. **120**, 147001 (2018).
[6]F. Onufrieva and P. Pfeuty, Phys. Rev. Lett. **102**, 207003 (2009).
[7]T. C. Song, X. H. Cai, M. W. Y. Tu, X. O. Zhang, B. V. Huang, N. P. Wilson, K. L. Seyler, L. Zhu, T. Taniguchi, K. Watanabe, M. A. McGuire, D. H. Cobden, D. Xiao, W. Yao, and X. D. Xu, Science **360**, 1214 (2018).
[8]W. Y. Kim and K. S. Kim, Nat. Nanotechnol. **3**, 408 (2008).
[9]F. Muñoz-Rojas, J. Fernández-Rossier, and J. J. Palacios, Phys. Rev. Lett. **102**, 136810 (2009).
[10]X. Y. Dong, D. Y. Zheng, M. Yuan, Y. R. Niu, B. B. Liu, and H. Wang, Phys. Rev. Appl. **13**, 064050 (2020).
[11]X. Y. Dong, D. Y. Zheng, and H. Wang, Adv. Electron. Mater. **5**, 1800844 (2019).
[12]Z. C. Zhao, H. Wang, S. Q. Xiao, D. Huang, Y. Z. Gu, Y. X. Xia, Q. Y. Jin, C. L. Zha, and X. S. Wu, J. Appl. Phys. **99**, 08R507 (2006).
[13]K. Szot, W. Speier, G. Bihlmayer, and R. Waser, Nat. Mater. **5**, 312 (2006).
[14]R. Waser and M. Aono, Nat. Mater. **6**, 833 (2007).
[15]A. H. Dong, K. Chang, R. Z. Wang, D. Y. Zheng, and H. Wang, Appl. Phys. Lett. **117**, 072104 (2020).
[16]Z. Gan, B. Zou, P. Zhou, X. Huang, C. Mei, and H. Wang, Nanotechnology **30**, 175201 (2019).
[17]X. Huang, K. A. Jiang, Y. R. Niu, R. Z. Wang, D. Y. Zheng, A. H. Dong, X. Y. Dong, C. L. Mei, J. Lu, S. Liu, Z. K. Gan, N. Zhong, and H. Wang, Appl. Phys. Lett. **113**, 112103 (2018).
[18]J. Lu, Z. Li, G. Yin, M. Ge, D. He, and H. Wang, J. Appl. Phys. **116**, 123102 (2014).
[19]K. S. Novoselov, A. K. Geim, S. V. Morozov, D. Jiang, Y. Zhang, S. V. Dubonos, I. V. Grigorieva, and A. A. Firsov, Science **306**, 666 (2004).
[20]X. Guo, W. Wang, H. Nan, Y. Yu, J. Jiang, W. Zhao, J. Li, Z. Zafar, N. Xiang, Z. Ni, W. Hu, Y. You, and Z. Ni, Optica **3**, 1066 (2016).
[21]B. K. Sarker, E. Cazalas, T.-F. Chung, I. Childres, I. Jovanovic, and Y. P. Chen, Nat. Nanotechnol. **12**, 668 (2017).
[22]S. K. Behura, C. Wang, Y. Wen, and V. Berry, Nat. Photonics **13**, 312 (2019).
[23]M. Lozada-Hidalgo, S. Zhang, S. Hu, V. G. Kravets, F. J. Rodriguez, A. Berdyugin, A. Grigorenko, and A. K. Geim, Nat. Nanotechnol. **13**, 300 (2018).
[24]B. C. Yao, S.-W. Huang, Y. Liu, A. K. Vinod, C. Choi, M. Hoff, Y. N. Li, M. B. Yu, Z. Y. Feng, D.-L. Kwong, Y. Huang, Y. J. Rao, X. F. Duan, and C. W. Wong, Nature **558**, 410 (2018).
[25]G. X. Ni, A. S. McLeod, Z. Sun, L. Wang, L. Xiong, K. W. Post, S. S. Sunku, B.-Y. Jiang, J. Hone, C. R. Dean, M. M. Fogler, and D. N. Basov, Nat. **557**, 530 (2018).
[26]C. Q. Yu and H. Wang, Adv. Mater. **22**, 966 (2010).
[27]C. Q. Yu and H. Wang, Appl. Phys. Lett. **97**, 041105 (2010).
[28]S. Liu, P. Cheng, and H. Wang, Opt. Lett. **37**, 1814 (2012).
[29]X. Xie, S. Liu, M. Z. Huang, and H. Wang, Opt. Express **23**, 24290 (2015).
[30]Z. K. Gan, B. Zhang, P. Q. Zhou, X. Huang, C. L. Mei, and H. Wang, Appl. Phys. Lett. **109**, 031106 (2016).
[31]Z. K. Gan, P. Q. Zhou, X. Huang, C. L. Mei, and H. Wang, Adv. Electron. Mater. **3**, 1700293 (2017).
[32]X. S. Li, W. W. Cai, J. H. An, S. Kim, J. Nah, D. X. Yang, R. Piner, A. Velamakanni, I. Jung, E. Tutuc, S. K. Banerjee, L. Colombo, and R. S. Ruoff, Sci. **324**, 1312 (2009).
[33]G. B. Barin, Y. Song, I. D. Gimenez, A. G. Souza, L. S. Barretto, and J. Kong, Carbon **84**, 82 (2015).
[34]K. Chang, X. Yu, B. Liu, Y. Niu, R. Wang, P. Bao, G. Hu, and H. Wang, IEEE Electron Device Lett. **42**, 824 (2021).
[35]X. Yu, K. Chang, A. Dong, Z. Gan, K. Jiang, Y. Ling, Y. Niu, D. Zheng, X. Dong, R. Wang, Y. Li, Z. Zhao, P. Bao, B. Liu, Y. Cao, S. Hu, and H. Wang, Appl. Phys. Lett. **118**, 172104 (2021).
[36]M. Yuan, X. Dong, Y. Niu, B. Liu, X. Chen, D. Zheng, A. Dong, and H. Wang, Nanotechnol. **31**, 405301 (2020).
[37]S. Liu, M. Huang, Y. Yao, H. Wang, K. Jin, P. Zhan, and Z. Wang, ACS Appl. Mater. Interfaces **7**, 19536 (2015).
[38]H. Wang, S. Q. Xiao, C. Q. Yu, Y. X. Xia, Q. Y. Jin, and Z. H. Wang, New J. Phys. **10**, 093006 (2008).
[39]L. Z. Kong, H. Wang, S. Q. Xiao, J. J. Lu, Y. X. Xia, G. J. Hu, N. Dai, and Z. H. Wang, J. Phys. D: Appl. Phys. **41**, 052003 (2008).
[40]S. Zhong, Z. Huang, X. Lin, Y. Zeng, Y. Ma, and W. Shen, Adv. Mater. **27**, 555 (2015).
[41]A. Polman, Sci. **322**, 868 (2008).